PREPRINT: Proceedings of IEEE GLOBECOM 2011, Houston, TX, USA, December 49, 2011

A Top-Down Random Generator for the In-Home PLC Channel

Andrea M. Tonello*, Fabio Versolatto*, and Benjamin Béjar†
* DIEGM - Università di Udine - Via delle Scienze 208 - 33100 Udine - Italy
e-mail: {tonello, fabio.versolatto}@uniud.it
† Universidad Politécnica de Madrid, Dpto. Seãles, Sistemas y Radiocomunicaciones
Avd. Complutense s/n, E.T.S.I. de Telecomunicación, 28040 Madrid
e-mail: min@gaps.ssr.upm.es

***Abstract*—We propose a random channel generator for in-home power line communications (PLC). We follow a statistical top-down approach and we model the multipath propagation effects of the PLC channel in the frequency domain. Then, we introduce the variability into the model, i.e., we let the parameters associated to the reflections be random, according to a certain statistics. Finally, we fit the model to the experimental data. We target the average path loss and root-mean-square (RMS) delay spread of the measured channels. According to this methodology, we show that the randomly generated channels are in good agreement with the experimental ones in terms of the main metrics.**

I. Introduction

Power line communications aims to deliver high-speed data content by exploiting the existent power delivery infrastructure. In the in-home scenario, where the power delivery network is widespread, PLC is able to overcome the range limitations of wireless networks ensuring high speed communications, namely, up to 200 Mbps [1].

A lot of research activity has been done in PLC channel modeling. However, no reference model has been provided yet. In this respect, two approaches are followed. The first is referred to as bottom-up approach. The bottom-up approach exploits the transmission line theory to compute the channel response between the transmitter and the receiver. It ensures strong connections with the reality since it uses all the topological information, but it is quite computationally expensive if applied to real PLC networks. Bottom-up models have been reported in [2], [3] and [4].

The second approach is commonly referred to as top-down. Basically, according to the top-down approach, the channel response is obtained by fitting a certain parametric function with measured data. Both the top-down and bottom-up approaches admit a statistical extension that allow for the random channel generation. Bottom-up random channel generators have been presented in [5], and more recently in [6] - [7]. Top-down random channel generators have been proposed in [8] - [9]. Furthermore, a comparison of the performance of different PLC channel generation algorithms has been done in [10].

In this work, we present a top-down random channel generator that has been partially described in [11] - [12]. We start from the mutipath propagation model. We derive an analytical expression of the channel frequency response that models the reflections in two-conductor transmission lines. Then, by letting some parameters be random according to a given statistics, we obtain a top-down random channel generator. We fit the model to the experimental data. In detail, we propose to target the average path loss and RMS delay spread of the measured data. Then, we study the statistics of the RMS delay spread, the average channel gain (ACG) and the coherence bandwidth of the simulated channels.

The work is organized as follows. In Section II, we derive the top-down random channel generator. We discuss the multipath propagation model and we present its statistical extension. In Section III, we provide some details of the fitting procedure. Then, in Section IV, we show the numerical results which validate the simulation approach that we have followed. Finally, the conclusions are reported in Section V.

II. Model Description

We now present the top-down random PLC channel generator. We assume the channel to be linear time-invariant. We firstly model the multipath effects and we provide an analytical expression of the PLC channel frequency response. Then, we simplify the general expression and finally we describe the statistics of the random parameters.

A. Deterministic Frequency Response Model

We consider the propagation of a signal over a two-conductor transmission line. We assume the line to be surrounded by a homogeneous dielectric, and the transversal dimension of the overall cable structure to be relatively small w.r.t. the transmission signal wavelength in the range of frequencies that we consider. Therefore, we make the transverse electromagnetic (TEM) or quasi-TEM mode assumption. We point out that the previous assumptions make the propagation problem treatable, though they simplify the reality.

The work of A. M. Tonello and F. Versolatto was partly supported by the EU FP7 project OMEGA - Home Gigabit Network. The work of B. Béjar was supported in part by the Spanish Ministry of Science and Innovation under the grant TEC2009-14219-C03-01.

We use the phasor representation for the electrical quantities. We refer to $V_{tx}(f)$ and $V_{rx}(f)$ as the voltage phasor vector at the transmitter and the receiver node, where f denotes the frequency.

Now, power line networks are characterized by the presence of branches and unmatched loads that can be modelled as line discontinuities. In correspondence of a line discontinuity, the signal is partially reflected toward the transmitter and it is partially transmitted over the discontinuity. Therefore, the discontinuity is characterized by a reflection coefficient $\rho(f)$ and a transmission coefficient $\tau(f)$. In the presence of multiple discontinuities, several copies of the transmitted signal propagate through the line toward the receiver. Each copy encounters different reflections and thus it follows a different path. Therefore, at the receiver side the signal can be written as the sum of N copies of the transmitted signal, i.e., [13]

$$V_{rx}(f) = \sum_{i=1}^{N} \underbrace{\left(\prod_{k=1}^{R_i} \rho_k(f) \prod_{l=1}^{T_i} \tau_l(f) \right)}_{p_i(f)} e^{-\gamma(f)\ell_i} V_{tx}(f)\,, \quad (1)$$

where R_i, T_i, ℓ_i are the number of reflection coefficients, the number of transmission coefficients, and the length of the i-th path, respectively, while $\gamma\,(f)$ is the propagation constant of the line. In general, the propagation constant is complex and it is given by the sum of the attenuation constant $\alpha(f)$ and the phase constant $\beta(f)$, i.e., $\gamma(f) = \alpha(f) + j\beta(f)$. Furthermore, we refer to the product of reflection and transmission coefficients of the i-th path as the path gain $p_i(f)$.

We denote with $H(f) = V_{rx}(f)/V_{tx}(f)$ the ratio between the phasor of the received signal and the phasor of the transmitted signal. Finally, we point out that $H(f)$ is equal to the channel frequency response (insertion loss). Therefore, it follows that [14]

$$H(f) = \sum_{i=1}^{N} p_i(f) e^{-(\alpha(f)+j\beta(f))\ell_i} \quad 0 \le B_1 \le f \le B_2\,, \quad (2)$$

where B_1 and B_2 determine the considered frequency band.

From now on, we focus on the analytic signal and thus we express the insertion loss in terms of Fourier transform.

B. Simplified Model

According to the experimental evidences, we herein simplify the general expression of the insertion loss provided in (2). We firstly focus on the path gains. The path gains are given by the product of multiple reflection and transmission coefficients. The transmission and reflection coefficients are always smaller than one in absolute value. We further assume them to be real-valued. Moreover, we propose to explicit the frequency dependence of the path gains as follows

$$p_i(f) = g_i + c_i f^{K_2}\,, \quad (3)$$

where g_i, c_i and K_2 do not depend on the frequency. We note that the frequency dependence for the path gains can be neglected by simply letting $c_i = 0$.

Now, we focus on the propagation constant. Powerline cables are not ideal transmission lines. They introduce losses that can be taken into account by the attenuation constant $\alpha(f)$. We model the attenuation constant as follows [14]

$$\alpha(f) = \alpha_0 + \alpha_1 f^K\,, \quad (4)$$

where α_0, α_1 and K are constant coefficients that depend on the characteristics of the power line cable. Conversely, we neglect non idealities in the definition of the phase constant. Hence, we model $\beta(f)$ as

$$\beta(f) = \frac{2\pi f}{\nu}\,, \quad (5)$$

where $\nu = c/\varepsilon_r$ is the propagation speed of the transmission line, c is the speed of the light in the vacuum, and ε_r is the relative dielectric constant of the insulator surrounding the conductors. We choose a value of the dielectric constant that models the non-uniform mixture of air and plastic that constitutes the dielectric in real networks. In detail, we set $\varepsilon_r = 1.5$, and thus $\nu = 2 \cdot 10^8 m/s$. Finally we focus on the number of paths N. The number of paths is in general infinite. However, the reflection and the transmission coefficients are smaller than one in absolute value. It follows that the path gains converge to 0 as the number of reflections increase. In this respect, we neglect paths characterized by small path gains and we limit the sum in (2) to the finite number of paths N_p.

C. Statistical Extension of the Model

The simplified expression derived in the previous section allows for the generation of a given insertion loss once the parameters have been specified. In general, the values of the parameters are obtained from the fitting of the measured data. This approach is commonly referred to as deterministic top-down.

We extend the deterministic top-down approach in statistical terms by introducing the variability into the parameters. We proceed as follows. We let the path gains, the path lengths and the number of paths be random variables. Then, we define their statistics. We firstly focus on the path gains. For $f \in [B_1, B_2]$, we model the reflection and the transmission coefficients as the product of a random sign flip $\xi \in \{-1, 1\}$ and a uniform distributed random variable $u \sim \mathcal{U}(0, 1]$. Note that $0 < u \le 1$, and thus we do not consider reflection or transmission coefficients equal to 0. We further assume ξ and u to be independent. It follows that the path gains are the product of random sign flips and uniformly distributed random variables. Since the product of uniformly distributed random variables tends to the log-normality, we model both g_i and c_i as a log-normal variable multiplied by a random sign flip. We assume g_i and c_i to be independent. We point out that due to the sign flip, g_i and c_i have zero mean, and we indicate their variances with σ_g^2 and $\sigma_c^2 = b_0^2 \sigma_g^2$, respectively. Without any loss of generality, we assume $\sigma_g^2 = 1$ and we multiply (2) by a constant factor A that allows for gain adjustments.

We assume the path lengths to be uniformly distributed in $[0, L_{max}]$ and the number of paths to be distributed as a

Poisson variable with mean ΛL_{max}. We note that the model corresponds to a Poisson process with intensity $\Lambda\,(paths/m)$ in the interval of length L_{max}, where the paths are the arrivals of the process. We point out that this model is not strictly amenable to experimental observations. However, it ensures that the resulting insertion loss statistically fits the reality, as it will be shown. Furthermore, it provides an analytical expression of the path loss which is used in the fitting process (see Section IV). We condition N_p to be at least one. Therefore, the probability mass function of N_p is given by

$$P\left(N_p = k | N_p > 0\right) = \frac{\left(\Lambda L_{max}\right)^k}{k!} \frac{e^{-\Lambda L_{max}}}{1 - e^{-\Lambda L_{max}}}, \quad (6)$$

where $k \geq 1$. We assume all the other parameters in (2) to be constant. In the next section, we detail how to extract their value from the measured data. Finally, the complete expression of the insertion loss is

$$H(f) = A \sum_{i=1}^{N_p} \left(g_i + c_i f^{K_2}\right) e^{-\left(\alpha_0 + \alpha_1 f^K\right)\ell_i} e^{-j\frac{2\pi f}{\nu}\ell_i}. \quad (7)$$

Under certain assumptions, it is possible to obtain the complex impulse response of the channel in a closed expression. In detail, by letting $c_k = 0\ \forall k$, and $K = 1$, from (7) we obtain

$$h(t) = A \sum_{i=1}^{N_p} \sum_{k=1}^{2} g_i e^{-\alpha_0 \ell_i} \frac{(-1)^{k-1}\, e^{\left(jt - \left(\frac{\alpha_1}{2\pi} + j\frac{1}{\nu}\right)\ell_i\right)\omega_k}}{\alpha_1 \ell_i + j2\pi\left(\frac{\ell_i}{\nu} - t\right)}, \quad (8)$$

where $\omega_k = 2\pi B_k$ and $t \geq 0$. When the assumptions are no longer valid, the complex impulse response has to be computed by means of inverse discrete Fourier transform (IDFT).

Now, we study the statistics of the insertion loss. We define the statistical power of the insertion loss as $P\left(f\right) = E\left[H(f)H^*(f)\right]$, where the superscript $\{\cdot\}^*$ denotes the complex conjugate, and $E\left[\cdot\right]$ denotes the expectation w.r.t. the random parameters, i.e., the path gains, the path lengths and the number of paths. In the following, we refer to $P(f)$ as the path loss. According to the statistical distributions of the parameters, and from (7), we obtain

$$P\left(f\right) = |A|^2 \frac{\Lambda\left(1 + b_0^2 f^{2K_2}\right)}{\left(1 - e^{-\Lambda L_{max}}\right)} \frac{1 - e^{-2\left(\alpha_0 + \alpha_1 f^K\right)L_{max}}}{2\left(\alpha_0 + \alpha_1 f^K\right)}. \quad (9)$$

III. Fitting of Real Channels

We aim to find the values of the constant parameters in (7). According to the deterministic top-down approach, we propose to fit a set of measured channels. We proceed as follows. We compute the average path loss of the measured channels. Then, we find the set of values of the parameters in (7) that ensures the minimum mean squared error between the average path loss of the measured channels and the analytical path loss in (9). We further constraint the minimization to target the mean delay spread of the measured channels. We define the delay spread in Section IV. Once the constant parameters have been obtained, we are able to generate channel responses that show, on average, the same statistics of the measured set. With this method, we show that the convergence is not only provided in terms of the mean value of the delay spread and the path loss. Rather, it also applies to the complete statistical distribution of the delay spread and the average channel gain, and to the mean value of the coherence bandwidth, as it will be shown in the next section.

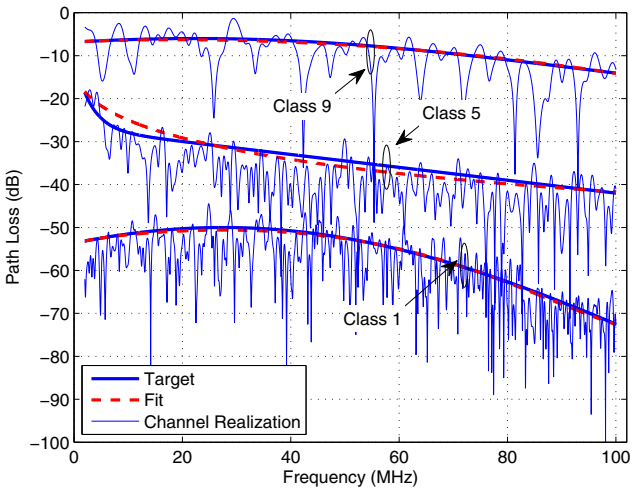

Fig. 1. Target path loss, fitted path loss and channel realizations of class 1 (bottom), class 5 (middle), and class 9 (top).

IV. Numerical Results

We firstly find the values of the simulator parameters starting from a set of measured data. Then, we study the statistics of the simulated channels in terms of the main metrics. We focus on the results of the large measurement campaign in [8], [15]. In [8], in-home PLC channels have been partitioned into nine classes. The classification has been made in terms of channel capacity, and the capacity has been computed under the assumption of additive white Gaussian background noise. We point out that the noise in PLC is not white. However, the classification allows to sort the channels according to their frequency behaviour. Each channel class is characterized by an average channel capacity, and further it shows its own statistics in terms of path loss, delay spread, and coherence bandwidth. The mean value of these metrics has been provided for all the nine classes in [16].

To prove the validity of the simulation approach, we focus on three of the nine classes, e.g., class 1, class 5 and class 9, in the $2-100$ MHz frequency band. Therefore, $B_1 = 2$ MHz, and $B_2 = 100$ MHz. We fit the experimental data according to the method of Section III and the results in [8], [16]. Hence, we report the optimal value of the parameters in Tab. I. In Fig. 1, we compare the target path loss obtained from experimental data (Target) to the simulated one (Fit). The target profile is the result of fitting with sinusoidal or exponential functions the mean path loss of measured channels [8]. A simulated channel realization is also shown for each class. We highlight the close matching between the target and the fitted path loss, which proves the fitting accuracy.

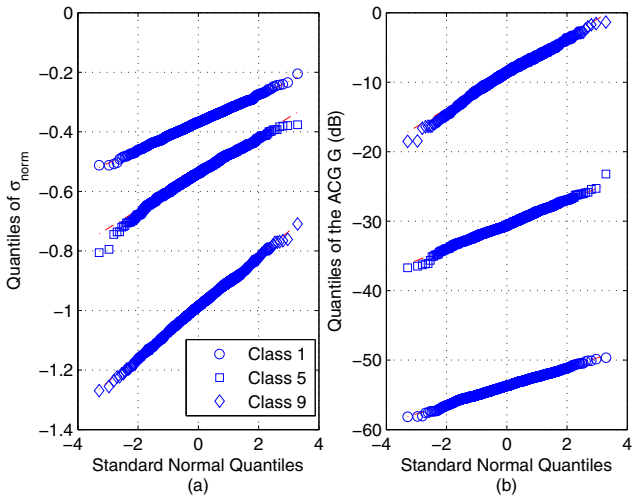

Fig. 2. On the left, QQ-plot of the normalized logarithmic delay spread (σ_{norm}). On the right, QQ-plot of the average channel gain (G).

Now, we focus on the statistical metrics. We generate 1000 channel realizations of each channel class. Then, we compute the RMS delay spread, the average channel gain and the coherence bandwidth of each channel realization. We firstly study the RMS delay spread. The RMS delay spread accounts for the energy spread of the channel impulse response. It is computed starting from the real channel impulse response $g(t) = 2\mathrm{Re}\{h(t)\}$, and the power delay profile

$$P(t) = \frac{|g(t)|^2}{\int_0^{+\infty} |g(\tau)|^2 \, d\tau} \tag{10}$$

as follows

$$\sigma_{RMS} = \sqrt{\int_0^{+\infty} (\tau - m_\tau)^2 \, P(\tau) \, d\tau} \quad (s), \tag{11}$$

where $m_\tau = \int_0^{+\infty} \tau P(\tau) \, d\tau$ is the mean delay. We compute the real channel impulse response by means of IDFT from (7). Furthermore, we truncate the impulse response at $5.56 \, \mu s$ in order to reduce the side-lobe effect.

In Table II, we compare the simulated and the experimental average delay spread of each class, namely, $\overline{\sigma}_{RMS}$. Again, the close matching proves the accuracy of the fitting process. We further investigate the distribution of the RMS delay spread. To this aim, we define the normalized logarithmic delay spread as $\sigma_{norm} = \log(\sigma_{RMS}/1\mu s)$. In Fig. 2a, we compare the quantiles of σ_{norm} to the quantiles of the standard normal distribution for all the channel classes. We have found that in all cases the samples lie on the robust linear fit line. Hence, σ_{norm} is normally distributed with good approximation, and thus, σ_{RMS} is log-normally distributed. This result is in accordance with the experimental evidence [9]. Furthermore, we point out that it does not depend on the fitting procedure, since the procedure targets only the average value of RMS delay spread.

Now, we address the statistics of the average channel gain. We focus on the dB version of the ACG, that is defined as follows

$$G = 10 \log_{10} \left(\frac{1}{B_2 - B_1} \int_{B_1}^{B_2} |H(f)|^2 \, df \right) (dB). \tag{12}$$

We compute the ACG of all the generated channels. Then, in Table II, we report the mean value for each class, namely $\overline{G}$, while in Fig. 2b we compare the quantiles of G to the standard normal quantiles. In accordance with the experimental evidence [9], we have found that the simulated G is normally distributed with good approximation for all classes. We further investigate the relation between the RMS delay spread and the ACG. In Fig. 3, we show the scatter plot of the RMS delay spread versus the ACG of the channel realizations of all three classes and we address the robust fit. We have found that the ACG and the RMS delay spread are negatively correlated on average, and the slope of the robust regression fit is $-0.048 \, \mu s/dB$. This result is in good agreement with the literature [9]. Clearly, to catch the entire variability of in-home channels, all nine classes should be considered together with their occurence probability.

Finally, we study the coherence bandwidth. To this aim, we define the correlation function of the frequency response as

$$R(\lambda) = \int_{-\infty}^{+\infty} H(f) \, H^*(f + \lambda) \, df. \tag{13}$$

We note that the correlation function is maximum for $\lambda = 0$. Then, we define the coherence bandwidth of the channel at the level $\varphi \in (0, 1)$ as the frequency B_c^{φ} for which the absolute value of the correlation function falls to a value φ times its maximum, i.e.,

$$B_c^{\varphi} = \lambda \quad \text{s.t.} \quad |R(\lambda)| = \varphi \, |R(0)| \tag{14}$$

TABLE I
PARAMETERS FOR CLASSES 1, 5 AND 9 [15],[16].

Parameter (unit)	Class 1	Class 5	Class 9
L_{max} (m)	580	280	130
Λ $(path/m)$	0.2	0.2	0.2
α_0 (m^{-1})	-0.0064	-0.0179	-0.0281
α_1 $(s \cdot m^{-1})$	9.9240e-27	1.9962e-5	2.4875e-20
K	2.9843	0.3654	2.2005
K_2	0.4039	-	0.3415
A	2.1763e-5	0.0016	0.0108
b_0^2	1.44e-6	0	2.25e-6

TABLE II
MEAN VALUES OF THE METRICS FOR CLASSES 1, 5, 9 [15],[16].

Class	Measured	Simulated		
	$\overline{\sigma}_{RMS}$ (μs)	$\overline{\sigma}_{RMS}$ (μs)	$\overline{G}$ (dB)	$\overline{B}_c^{0.9}$ (kHz)
1	0.31	0.43	-53.7	196.6
5	0.32	0.29	-30.5	276.8
9	0.04	0.10	-8.8	909.2

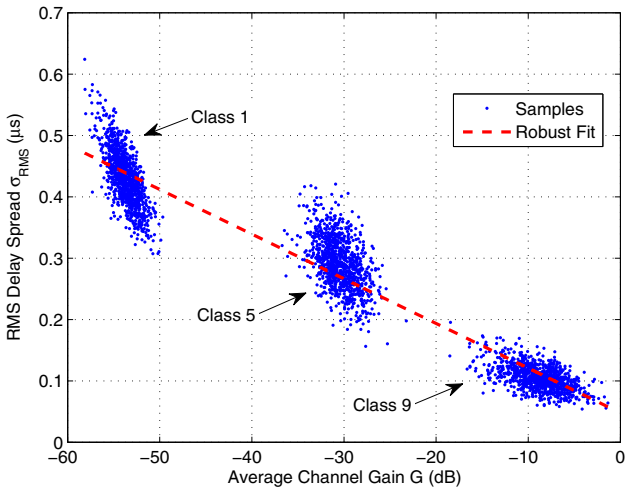

Fig. 3. Scatter plot of the RMS delay spread versus the average channel gain.

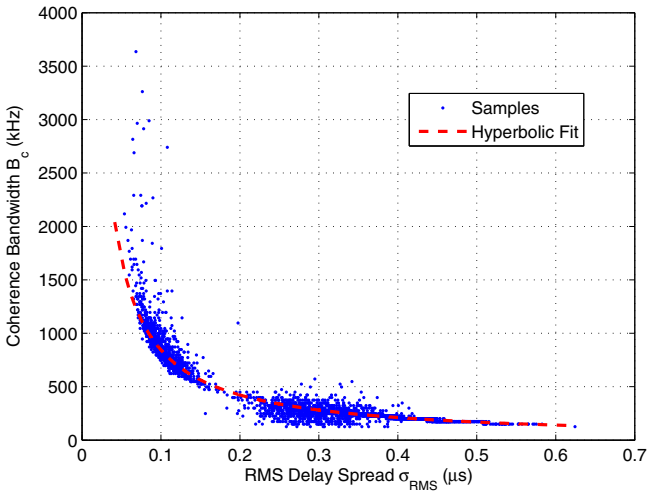

Fig. 4. Scatter plot of the coherence bandwidth versus the RMS delay spread.

We set $\varphi = 0.9$ and we compute $B_c^{0.9}$ for all channel realizations. In Table II, we report the average value of the coherence bandwidth for each channel class, i.e., $\overline{B}_c^{0.9}$. Further, we investigate the relation between the coherence bandwidth and the RMS delay spread. In Fig. 4, we show the scatter plot of the coherence bandwidth versus the RMS delay spread of all the channel realizations. The best fit is given by the hyperbolic curve that reads $B_c^{0.9} = 0.084/\sigma_{RMS}$. This relation is not far from the one obtained from the measured data [16]. Again, this proves the validity of the top-down statistical approach that we propose.

V. Conclusions

We have presented a top-down statistical approach that allows for the random channel generation. We have firstly described the multipath propagation model. Then, we have simplified the model and we have introduced the variability into a restricted set of parameters. Finally, we have proposed to fit the model to a set of measured data. To this aim, we focused on the average path loss and the RMS delay spread. The validity of this approach has also been shown. In detail, we have fitted three sets of measured channels for which the values of the main metrics are available in the literature. We have shown that simulated channels have the same path loss and delay spread, on average, of the measured channels. This validates the fitting process. Further, we have studied the statistics of the delay spread, the average channel gain and the coherence bandwidth of the generated channels. We have found strong connections with the experimental data. We point out that this aspect is not strictly due to the fitting process. Rather, it proves that the analytical expression that we have proposed for the random channel generation, is effectively able to model the nature of the PLC channels.

References

[1] Home Plug Alliance. [Online]. Available: www.homeplug.org

[2] A. M. Tonello and T. Zheng, "Bottom-Up Transfer Function Generator for Broadband PLC Statistical Channel Modeling," in *Proc. IEEE Int. Symp. Power Line Commun. and Its App. (ISPLC)*, Apr. 2009, pp. 7–12.

[3] S. Galli and T. C. Banwell, "A Deterministic Frequency-Domain Model for the Indoor Power Line Transfer Function," *IEEE J. Sel. Areas Commun.*, vol. 24, no. 7, pp. 1304–1316, Jul. 2006.

[4] F. J. Cañete, J. A. Cortés, L. Díez, and J. T. Entrambasaguas, "Broadband Modelling of Indoor Power-Line Channels," *IEEE Trans. Consum. Electron.*, vol. 48, no. 1, pp. 175–183, Feb. 2002.

[5] T. Esmailian, F. R. Kschischang, and P. Glenn Gulak, "In-Building Power Lines as High-Speed Communication Channels: Channel Characterization and a Test Channel Ensemble," *Intern. J. of Commun. Syst.*, vol. 16, no. 5, pp. 381–400, jun 2003.

[6] A. M. Tonello and F. Versolatto, "Bottom-Up Statistical PLC Channel Modeling - Part I: Random Topology Model and Efficient Transfer Function Computation," *IEEE Trans. Power Del.*, vol. 26, no. 2, pp. 891–898, Apr 2011.

[7] A. M. Tonello and F. Versolatto, "Bottom-Up Statistical PLC Channel Modeling - Part II: Inferring the Statistics," *IEEE Trans. Power Del.*, vol. 25, no. 4, pp. 2356–2363, Oct. 2010.

[8] M. Tlich, A. Zeddam, A. Moulin, and F. Gauthier, "Indoor Power-Line Communications Channel Characterization Up to 100 MHz - Part I: One-Parameter Deterministic Model," *IEEE Trans. Power Del.*, vol. 23, no. 3, pp. 1392–1401, July 2008.

[9] S. Galli, "A Simplified Model for the Indoor Power Line Channel," in *Proc. IEEE Int. Symp. Power Line Commun. and Its App. (ISPLC)*, Apr. 2009, pp. 13–19.

[10] F. J. Cañete, J. A. Cortés, L. Díez, and J. L. G. Moreno, "On the Statistical Properties of Indoor Power Line Channels: Measurements and Models," in *Proc. IEEE Int. Symp. Power Line Commun. and Its App. (ISPLC)*, Apr. 2011, pp. 271–276.

[11] A. M. Tonello, "Wideband Impulse Modulation and Receiver Algorithms for Multiuser Power Line Communications," *EURASIP Journal on Advances in Signal Processing*, vol. 2007, pp. 1–14.

[12] A. M. Tonello, S. D'Alessandro, and L. Lampe, "Adaptive Pulse-Shaped OFDM with Application to In-Home Power Line Communications," *IEEE Trans. Commun.*, vol. 58, no. 11, pp. 3265–3276, Nov. 2010.

[13] D. Anastasiadou and T. Antonakopoulos, "Multipath Characterization of Indoor Power-Line Networks," *IEEE Trans. Power Del.*, vol. 20, no. 1, pp. 90–99, Jan. 2005.

[14] M. Zimmermann and K. Dostert, "A Multipath Model for the Powerline Channel," *IEEE Trans. Commun.*, vol. 50, no. 4, pp. 553–559, Apr. 2002.

[15] F.P.7 Theme 3 ICT-213311 OMEGA, "PLC Channel Characterization and Modelling," Deliverable 3.2, Dec. 2008.

[16] M. Tlich, A. Zeddam, A. Moulin, and F. Gauthier, "Indoor Power-Line Communications Channel Characterization up to 100 MHz - Part II: Time-Frequency Analysis," *IEEE Trans. Power Del.*, vol. 23, no. 3, pp. 1402–1409, July 2008.